A EUROPEAN JOURNAL OF CHEMICAL BIOLOGY

CHEMBIOCHEM

SYNTHETIC BIOLOGY & BIO-NANOTECHNOLOGY

Accepted Article

Title: Co-evolving the Activity and Thermostability of an ε-Ketoester Reductase for Better Synthesis of (R)-α-Lipoic Acid Precursor

Authors: Yao Xu, Qi Chen, Zhi-Jun Zhang, Jian-He Xu, and Gao-Wei Zheng

To be cited as: *ChemBioChem* 10.1002/cbic.201900693

Link to VoR: http://dx.doi.org/10.1002/cbic.201900693

A Journal of ChemPubSoc Europe

WILEY-VCH www.chembiochem.org

Co-evolving the Activity and Thermostability of an ε-Ketoester Reductase for Better Synthesis of (*R*)-α-Lipoic Acid Precursor

Yao Xu,[a] Qi Chen,[a] Zhi-Jun Zhang,[a] Jian-He Xu,[a] and Gao-Wei Zheng*[a]

Abstract: In this work, we identified a significantly improved variant S131Y/Q252I of natural ε-ketoester reductase *Cp*AR2 from *Candida parapsilosis* for efficient manufacturing (*R*)-ECHO [(*R*)-8-chloro-6-hydroxyoctanoate] by co-evolving the activity and thermostability. The activity of variant $CpAR2_{S131Y/Q252I}$ towards ε-ketoester ethyl 8-chloro-6-oxooctanoate was improved to 214 U mg^{-1} from 120 U mg^{-1} of the wild-type enzyme ($CpAR2_{WT}$), and the half-deactivating temperature (T_{50}, for 15 min incubation) was simultaneously increased by 2.3°C compared with $CpAR2_{WT}$. Consequently, only 2 g L^{-1} of lyophilized *E. coli* cells harboring $CpAR2_{S131Y/Q252I}$ and glucose dehydrogenase (GDH) were required to achieve a similar productivity (530 g L^{-1} d^{-1}) of our previous work under the optimized reaction conditions. This result demonstrated a more economical and efficient process for the production of the key (*R*)-α-lipoic acid intermediate.

Introduction

α-Lipoic acid is a kind of safe and potent chiral antioxidant that can be used as dietary supplement and for treatment of diabetic neuropathy[1] and nephropathy,[2] although only its *R*-enantiomer shows the desired bioactivity[3]. Nowadays, most of the products available commercially are still produced and employed in a form of racemic mixture, because the inactive *S*-enantiomer did not show any obvious side effect,[4] and the price of the single *R*-enantiomer is as much as five times that of the racemate. Nevertheless, in order to reduce the metabolic burden of the human body, it is highly desired to develop a green and efficient method to asymmetrically synthesize the enantiomerically pure (*R*)-α-lipoic acid, instead of tedious and eco-unfriendly diastereomeric resolution of the chemically synthesized racemate, which is currently used in industry.[5]

Although numerous routes have been developed for the synthesis of (*R*)-α-lipoic acid,[5,6] they are constrained by some issues, including the maximum theoretical yield of 50% (kinetic resolution), the complex synthetic process, and the generally inadequate stereoselectivity (requiring the additional processes to upgrade the optical purity of product). Biocatalytic asymmetric reduction of ethyl 8-chloro-6-oxooctanoate (1, ECOO) developed recently is a reliable, straightforward and easy to up-scale route to the key precursor ethyl (*R*)-8-chloro-6-hydroxyoctanoate (2, (*R*)-ECHO) for introduction of the chiral center into (*R*)-α-lipoic acid, which attracts widespread attention due to its advantages of 100% theoretical yield and simple operation process for the (*R*)-α-lipoic acid manufacture (Scheme 1).[7]

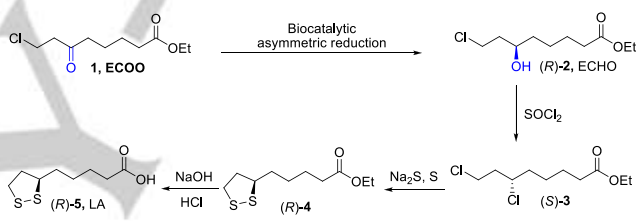

Scheme 1. Chemoenzymatic route for the asymmetric synthesis of (*R*)-α-Lipoic acid (LA).

However, the large scale application of these biocatalytic processes are limited by low substrate loading, poor conversion, or insufficient stereoselectivity and productivity. This is because the bulky and special structure of ε-ketoester substrate ECOO, making it more difficult to be reduced by ketoreductases compared with the well-studied α- or β-ketoesters.[8] This dramatically decreases the probability of hitting an active enzyme towards ECOO-like ε-ketoesters. Therefore, it is difficult to create an industrially feasible biocatalyst for green synthesis of (*R*)-ECHO, if considering the long distance between the ε-position of the carbonyl group accepting the hydride from NAD(P)H and the ester group positioned in the binding site of ketoreductases.

Recently, we identified an unusual ε-ketoester reductase *Cp*AR2 from *Candida parapsilosis*.[9] Using *Cp*AR2 as catalyst, (*R*)-ECHO with 99% ee was produced in a space-time yield (STY) of 530 g L^{-1} d^{-1} via the asymmetric reduction of ECOO, highlighting a particularly attractive and potential process for enzymatic synthesis of (*R*)-α-lipoic acid precursor. However, high biocatalyst loading (10 g L^{-1} of dry *E. coli* cells coexpressing *Cp*AR2 and a glucose dehydrogenase *Bm*GDH) is required to achieve such high STY in the bioreduction process, resulting in serious emulsification and tedious multi-step downstream processing to obtain high product isolated yield. For large scale application, a low biocatalyst loading is highly desired. It not only reduces cost contribution also avoids post-reaction processing issues (such as foaming or formation of

[a] *Y. Xu, Q. Chen, Dr. Z. J. Zhang, Prof. J. H. Xu, Prof. G. W. Zheng*
State Key Laboratory of Bioreactor Engineering, Shanghai Collaborative Innovation Center for Biomanufacturing Technology, East China University of Science and Technology, Shanghai 200237, China
E-mail: gaoweizheng@ecust.edu.cn

Supporting information for this article is given via a link at the end of the document.

emulsions during the extraction of product from water using organic solvents). Generally, the biocatalyst loading should be less than 5 g L^{-1} for a green and economical chemical process.[10]

Directed evolution has been proven to be an effective strategy for improving the performance of enzymes by mimicking natural evolution without the knowledge of protein structure-function relationships.[11] To reduce the biocatalyst loading, and meet or exceed the targets for the practical application, multiple enzyme features are need to be evolved simultaneously. Due to the excellent stereoselectivity (>99% ee) of *Cp*AR2, we here intend to improve its activity and thermal stability simultaneously. To avoid the frequently encountered tradeoff between different properties, we adopted a co-evolution strategy for identifying the overall improved variants but excluding those mutants with bias on any individual performance, either activity or stability, which is important to create promising biocatalysts of industrial potential.

Results and Discussion

To identify *Cp*AR2 variants with improved activity and thermostability, we first constructed a mutant library by error-prone PCR[12] using pET28a-*Cp*AR2 as a template, and performed an initial screening of approximately 4,000 bacterial clones with 1-4 mutated residues per clone on average. As a result, two potential hot spots, S131 and Q252, for enhancing both the activity and thermostability of *Cp*AR2 were identified through two rounds of epPCR-based random mutagenesis and subsequent high-throughput screening based on 96-well plate assay. A substrate-docking simulation also demonstrated that Ser131 is a residue surrounding the active site of *Cp*AR2, which might interact with the ester group of the substrate ECOO (within a distance of 6 Å) (Figure 1).

To further investigate the effect of all Ser131 mutations, we performed site-directed mutagenesis to replace Ser131 of *Cp*AR2 with 19 other canonial amino acids, and assayed the specific activity of all mutants. As shown in Figure 2, the mutation of Ser131 into Tyr, Phe, Met or Leu significantly improved the enzyme activity towards the ECOO. Among them, the best mutant S131Y showed a nearly 2-fold higher specific activity (237 U mg^{-1}) compared with the wild-type enzyme (120 U mg^{-1}). Therefore, mutations of Ser131 seemed effective in increasing the activity of *Cp*AR2, even though Ser131 has no direct interaction with the carbonyl group of the substrate. Interestingly, unlike the general case, in which the mutation of the residue near the active site into an amino acid with smaller side chain group usually enhances the catalytic efficiency due to the enlarged pocket and substrate channel.[13] Accordingly, the mutations Ser131Tyr and Ser131Phe with larger side chain containing a benzene ring exihibited the highest activity.

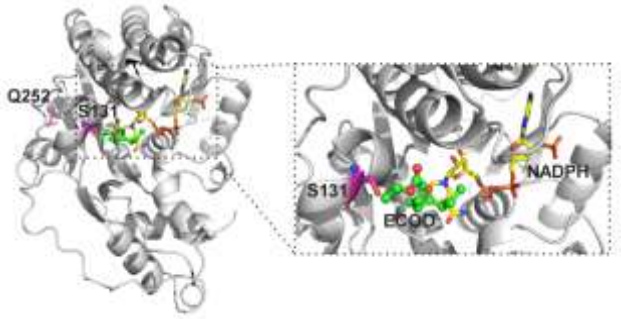

Figure 1. The locations of S131 and Q252 in the modelled structure of *Cp*AR2.

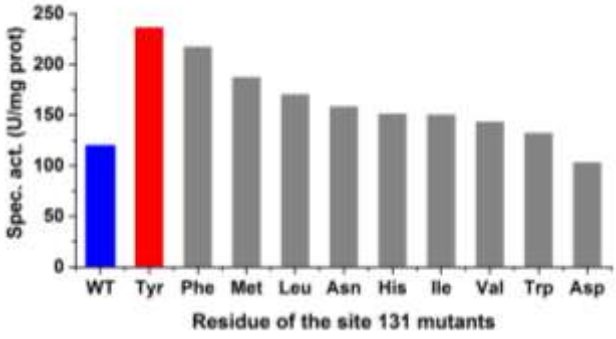

Figure 2. The specific activities of mutants at S131 position.

During the process of screening, we also noticed that a double mutant S131L/Q252I exhibited better thermostability than the mutants S131L and S131Y (Table 1), suggesting that the mutation of thermally labile residues (e.g., Gln, Asn, Asp, Cys) on the surface of protein molecules is effective to increase *Cp*AR2 thermostability.[14]

To elucidate the reason behind the enhanced specific activity of *Cp*AR2 variants towards ECOO, we performed a kinetic analysis as shown in Table 1. Specific activities of the purified variants S131Y and S131Y/Q252I measured were 237 U mg^{-1} and 214 U mg^{-1}, respectively, which are much higher than that of the wild-type *Cp*AR2 (120 U mg^{-1}). The k_{cat} of variant S131Y for ECOO reduction was up to 181 s^{-1}, 2-fold higher than that of the wild-type enzyme (90.1 s^{-1}), and K_m decreased slightly, resulting in an obviously increase in catalytic efficiency k_{cat}/K_m (255 s^{-1} mM^{-1} *vs* 77 s^{-1} mM^{-1}). The kinetic analysis revealed that the S131 is a key residue for improve k_{cat} of *Cp*AR2 towards ECOO, which contribute significantly to the increase of catalytic efficiency. In addition, these mutations have no effect on the stereoselectivity of *Cp*AR2. All variants afforded the (*R*)-ECHO with 99% ee.

Table 1. Properties of *Cp*AR2 and its variants towards substrate ECOO.

Enzyme	Specific activity (U mg^{-1})	k_{cat} (s^{-1})	K_m (mM)	k_{cat}/K_m (s^{-1} mM^{-1})	Half-life (h)[a]	T_{50}^{15} (°C)
WT	120	90.1	1.17	77	4.3	45.5
S131L	171	120 ± 6	0.95 ± 0.19	126	25.5	46.5
S131Y	237	181 ± 9	0.71 ± 0.10	255	24.8	46.8
S131L/Q252I	197	172 ± 7	1.05 ± 0.10	164	32.5	48.8
S131Y/Q252I	214	140 ± 3	0.65 ± 0.08	215	25.1	47.8

[a] Half-life of wide-type *Cp*AR2 and its mutants at 40°C.

The specific activity of variant S131Y/Q252I was increased to 214 U mg^{-1} from 120 U mg^{-1}. Moreover, the half-deactivating temperature (T_{50}^{15}) was 2.3°C higher than the wild-type enzyme, and the half-life of enzyme at 40°C were increased to more than 24 h from 4.3 h. To simplify the preparation of biocatalysts, we coexpressed *Cp*AR2$_{S131Y/Q252I}$ or *Cp*AR2$_{WT}$ and a glucose dehydrogenase *Bm*GDH[15] for NADPH regeneration in an *E. coli* cell according to previous reports.[9a] Then the whole cells of *E. coli* *Cp*AR2$_{WT}$/*Bm*GDH, *Cp*AR2$_{S131Y}$/*Bm*GDH and *Cp*AR2$_{S131Y/Q252I}$/*Bm*GDH as biocatalysts were used to perform the asymmetric reduction of ECOO.

With these biocatalysts in hand, we further evaluated the feasibility for their use in reduction of 110 g L^{-1} of ECOO at low biocatalyst loading. Using only 2 g L^{-1} of *Cp*AR2$_{S131Y/Q252I}$/*Bm*GDH or *Cp*AR2$_{S131Y}$/*Bm*GDH cells as catalyst, 110 g L^{-1} of ECOO was both completely converted within 5 h, providing (*R*)-ECHO with a similar space-time yield (Table 2, entries 2 and 3). In contrast, using the same amount *Cp*AR2$_{WT}$/*Bm*GDH cells as catalyst, only 68% substrate was reduced within 22 h (Table 2, entry 1). Subsequently, a simple reaction optimization was carried out. When 5% (v/v) DMSO instead of 5% (v/v) EtOH was used as cosolvent and the reaction temperature was reduced to 35°C from 40°C, the same amount substrate was completely converted within 4 h, providing a higher STY of 566 g L^{-1} d^{-1}, a similar productivity with our previous work [9a] but a 5-fold decrease in catalyst dosage. These results indicated that a more efficient engineered ε-ketoester reductase for the synthesis of (*R*)-α-lipoic acid precursor was developed by cooperative directed evolution. The green and economically viable bioreduction process has been applied to (*R*)-α-lipoic acid precursor production in 2000-L scale reactors by Suzhou Fushilai Pharmaceutical Co., Ltd (Suzhou, China).

Table 2. Asymmetric reduction of ECOO with lyophilized *E. coli* cells of *Cp*AR2$_{WT}$/*Bm*GDH and *Cp*AR2$_{S131Y/Q252I}$/*Bm*GDH.

Entry	Biocatalyst	Substrate loading (g L^{-1})	Enzyme loading (g L^{-1})	Time (h)	Conversion (%)[c]	Yield (%)	ee (%)[c]	STY (g L^{-1} d^{-1})
1	*Cp*AR2$_{WT}$/*Bm*GDH[a]	110	2	22	68	81	99	66
2	*Cp*AR2$_{S131Y}$/*Bm*GDH[a]	110	2	5	>99	84	99	448
3	*Cp*AR2$_{S131Y/Q252I}$/*Bm*GDH[a]	110	2	5	>99	85	>99	454
4	*Cp*AR2$_{S131Y/Q252I}$/*Bm*GDH[b]	110	2	4	>99	85	>99	566

[a] Reaction conditions: 0.5 M ECOO (110 g L^{-1}), 1.5 equiv. glucose, 2.0 g L^{-1} lyophilized *E. coli* cells harboring pET28a-*Cp*AR2/*Bm*GDH (*Cp*AR2$_{WT}$: 17.7 kU/g cells; *Cp*AR2$_{S131Y/Q252I}$: 32.1 kU/g cells; *Bm*GDH: 3.5 kU/g cells), NADP$^+$ (0.1 mM), 0.5 mL EtOH, and 9.5 mL Tris-HCl buffer (100 mM, pH 7.0), 40°C, with pH kept at 7.0 by auto-titrating 1.0 M K_2CO_3.

[b] Reaction conditions: 0.5 M ECOO (110 g L^{-1}), 1.5 equiv. glucose, 2.0 g L^{-1} lyophilized *E. coli* cells harboring *Cp*AR2$_{S131Y/Q252I}$/*Bm*GDH (*Cp*AR2$_{S131Y/Q252I}$: 32.1 kU/g cells; *Bm*GDH: 3.5 kU/g cells), NADP$^+$ (0.1 mM), 0.5 mL DMSO, and 9.5 mL Tris-HCl buffer (100 mM, pH 7.0), 35°C, with pH kept at 7.0 by auto-titrating 1.0 M K_2CO_3.

[c] Conversion and ee were determined by GC analysis.

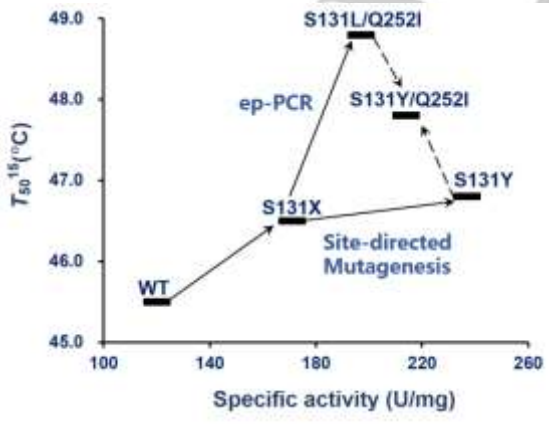

Figure 3. Scheme and results for the co-operative directed evolution of *Cp*AR2's activity and thermostability.

Conclusion

In summary, we performed the screening of a random mutation library of *Cp*AR2 for identifying an enzyme variant with high activity and thermostability. It was demonstrated that mutations at Ser131 and Gln252 contribute to the enhanced specific activity and thermostability, respectively. Among saturation mutants of S131, S131Y exhibited the highest specific activity for ECOO reduction. Kinetic analysis showed that its increased catalytic efficiency is largely attributable to the increased k_{cat}. Subsequently, the beneficial mutants were combined, achieving the best double mutant S131Y/Q252I. Its specific activity was 215 U mg^{-1}, and the half-deactivating temperature (T_{50}^{15}) was

2.3°C higher than the wild-type enzyme, resulting in 5-fold decrease in the enzyme loading (only 2 g dry engineered cells per liter) and obvious simplification of the post-reaction processing which would otherwise be very difficult in the case of high dosage of the interface active protein biocatalyst due to the severe emulsification issue often encountered during the extraction of product with organic solvents (Figure 3).

Experimental Section

Materials: The enzyme substrate, ethyl 8-chloro-6-oxooctanoate (ECOO), was provided by Suzhou Fushilai Medicine & Chemical Co., Ltd. (Jiangsu, China). All others chemicals and reagents were purchased from commercial suppliers. *E. coli* BL21 (DE3) was used as cloning and expression host. Cells were incubated in Luria-Bertani (LB) medium. The melting temperature (T_m) of enzyme was measured using circular dichroism. The oligonucleotide primers designed for mutagenesis were synthesized by Sangon Biotech Co. (Shanghai, China). Restriction enzymes were purchased from New England Biolabs (Beijing, China). PrimeSTAR® HS (Premix), Recombinant Taq DNA Polymerase (Taq™) and T4 DNA Ligase were purchased from TaKaRa (Dalian, China).

Random mutagenesis: The plasmid pET-28a containing *Cp*AR2-WT gene was used as the template for the construction of random mutant library. Error-prone PCR was performed with primers (Table S1) incorporating *Eco*RI and *Xho*I restriction sites. The PCR mixture (50 μL) was composed of pET28a-*Cp*AR2-WT DNA (<500 ng), 10 mM Tris-HCl (pH 8.3), 50 mM KCl, 1.5 mM $MgCl_2$, 0.2 mM each dNTPs mixture, 0.4 μM each of the two primers, and 0.5 μL DNA polymerases (5 U/μL). The PCR mixture was pre-incubated at 95°C for 3 min, then was cycled 30 times with the following program: 94°C for 10 s, 60°C for 30 s, and 72°C for 90 s. The amplified PCR product was purified with TRIpure Reagent Kit from Aidlab (Beijing, China), digested with *Eco*RI and *Xho*I, and ligated into the *Eco*R I and *Xho* I sites of pET-28a. The resultant recombinant plasmid was transformed into chemical competent *E. coli* BL21 (DE3) and plated onto Luria-Bertani (LB) agar plates containing 50 μg/mL kanamycin, and the plasmids extracted from the kanamycin-resistant colonies were used to isolate *Cp*AR2 mutants as the random library.

Site-directed mutagenesis: MEGAWHOP method (Megaprimer PCR of Whole Plasmid) was used to generate site-directed mutant with corresponding primers (Table S1). MEGAWHOP was carried out with a mixture (50 μL) containing 1 ng pET28a-*Cp*AR2-WT DNA, 0.25 μM each of the two degenerate primers (Table S1), 0.2 mM each dNTPs and 25 μL PrimeSTAR HS DNA Polymerase (1.25 U/25 μL). The PCR mixture was pre-incubated at 98°C for 3 min, and then subjected to thermal cycles (98°C for 10 s, 55°C for 5 s and 72°C for 6 min, 30 cycles). The resulting PCR product was digested with 1 μL *Dpn*I (37°C for 2 h). The cloned plasmids were then transformed into chemically competent *E. coli* BL21 (DE3) cells and plated on LB agar plates containing kanamycin (50 μg/mL). The resulting mutant plasmids were confirmed by DNA sequencing.

Screening of variants with improved activity and thermostability: Library colonies were picked with sterile toothpicks and inoculated into 200 μL LB medium containing 50 μg/mL kanamycin in 96-well plates, before incubated overnight at 37°C. The resulting cultures were inoculated into 400 μL LB medium containing kanamycin in new 96-well plates, and incubated at 37°C for 1.5−2.0 h. The protein expression was induced by adding 0.2 mM IPTG (final concentration) and then the incubation was continued at 16°C for another 24 h. Cells were lysed by adding 200 μL buffer containing lysozyme (750 mg/L) and DNase I (10 mg/L) and incubating at 37°C for 2 h. The plates were centrifuged at 2395×*g* and 4°C for 10 min. The supernatant was then subjected to activity and thermostability assay as follows: After 50 μL properly diluted supernatants from the deep-well plate were transferred to microtiter plates, the reduction reaction was initiated by adding 150 μL reaction mixture composed of 100 mM Tris-HCl buffer (pH 7.0), 0.2 mM NADPH and 2 mM substrate. The activity of variants was determined at 30°C by measuring the change of absorbance at 340 nm for 220 s using a microplate spectrophotometer (BioTek, USA). Each of the supernatants (20 μL) from the deep-well plates was transferred to 96-well PCR plates, heated at a defined temperature for 15 min, and followed by cooling on ice for 5 min. Each of the properly diluted supernatants (50 μL) from the pre-incubated 96-well PCR plates were transferred to a microtiter plate. Then the residual activity of each variant was measured using the microplate spectrophotometer under the standard assay condition. The variants with higher initial or residual activity than the parental enzyme were chosen for subsequent rescreening. The top mutants were confirmed by DNA sequencing and activity / thermostability assay of the purified enzymes.

Expression and purification of proteins: The *E. coli* BL21 (DE3) cells harboring the recombinant pET-28a(+) plasmids of *Cp*AR2-WT and its variants were cultivated overnight at 37°C in 4 mL LB medium containing 50 μg/mL kanamycin. The overnight culture was then inoculated into 100 mL LB and cultivated at 37°C and 180 rpm until the culture's optical density (OD_{600}) reaching 0.6−0.8. The protein expression was induced at 16°C with the addition of IPTG to a final concentration of 0.1 mM. After cultivation for 24 h, the cells were collected by centrifugation. For preparing the lyophilized cells, a portion of the cells was directly freeze-dried for 72 h. For protein purification, another portion of the cells were washed and resuspended in buffer A (20 mM sodium phosphate buffer, pH 7.4, 500 mM NaCl, 10 mM imidazole). The cell suspension was disrupted by ultrasonication, and centrifugated (13,000×*g*, 4°C, 40 min). Then the resulting supernatant was filtered through a 0.22 μm filter and then loaded into a standard Ni-NTA affinity column which was pre-equilibrated with ice chilled buffer A. The column was subsequently washed by elution buffer with an increasing gradient of imidazole from 10 to 500 mM, using the mixture of buffer A and buffer B (20 mM sodium phosphate

buffer, pH 7.4, 500 mM NaCl, 500 mM imidazole). The fractions containing the target protein was collected and concentrated by ultrafiltration using Ultra-4 centrifugal filter with 10 kDa cut off (Millipore, USA) and then washed three times by buffer C (25 mM Tris-HCl, 150 mM NaCl, 1 mM DTT). The purity of target protein was checked by SDS-PAGE (Figure S1). The purified protein was stored at −80°C for further use. Protein concentration of the purified enzyme was estimated by detecting the absorbance at 280 nm using a NanoDrop 2000c spectrophotometer (Thermo Scientific) and taking into account the calculated extinction coefficients with the ExPASy ProtParam Tool.

Enzyme assays: The reductase activity was assayed at 30°C by monitoring the decrease in the absorbance of NADPH at 340 nm within 1 min on a UV-spectrophotometer (Shimadzu, UV1800). The standard assay mixture (1 mL) was composed of 970 µL Tris-HCl buffer (100 mM, pH 7.0), 10 µL ethyl 8-chloro-6-oxooctanoate (800 mM), 10 µL NADPH (10 mM), and 10 µL enzyme with an appropriate concentration. One unit of enzyme activity (U) was defined as the amount of enzyme that can catalyze the oxidation of 1 µmol NADPH per minute under above conditions.

Kinetic properties: The kinetic parameters of the purified *Cp*AR2 were determined by measuring the activity at the different substrate concentrations (0.1−10 mM) and a fixed NADPH concentration. All data were handled by using the software OriginPro 9.0 to adjust to the Michaelis-Menton model (Figure S2).

Thermostability: The thermal stability of *Cp*AR2 was also examined by incubating the purified enzymes (1.0 mg mL^{-1}) at varied temperatures (44−49°C), and the residual activity was assayed as described above.

The half-deactivating temperature (T_{50}^{15}) was determined by measuring the residual activity after incubation at a gradient temperatures for 15 min. The T_{50}^{15} was estimated as temperature at which heat treatment for 15 min reduced the initial activity by 50%. The purified enzymes were diluted to 1.0 mg/mL and 20 µL each of the purified enzyme was distributed into 8 thin-walled PCR tubes, which were then subjected to incubation at a temperature gradient using a thermocycler (Bio-Rad, USA). After incubation, the PCR tubes were cooled on ice immediately. Then, the residual activities of the enzymes were measured with the standard protocol (Figure S3).

The melting temperature (T_m) of *Cp*AR2 were determined via circular dichroism (CD) spectroscopy. The concentration of initial protein samples was diluted to 0.3 mg/mL with 100 mM potassium phosphate buffer (pH 7.0). The CD spectra of the diluted samples were individually detected in a 0.2 cm-path-length cuvette using a Chirasan circular dichroism spectrograph (Applied Photophysics, UK) by scanning at 180-260 nm (1 nm/step) under increasing temperatures (35−65°C, 2°C/step, 2°C/min). Then the protein CD spectra measured as a function of temperature were analyzed using Global 3 analysis software (Applied Photophysics, UK) to obtain the calculated T_m values.

For the half-life determination, each of the purified enzymes (1.0 mg/mL) was incubated at 40°C. Aliquots were taken at specific time intervals and cooled on ice before activity assay, followed by measuring the residual activity using the standard activity assay method described above. The initial activity detected before incubation was normalized as 100%. The half-lives were determined according to first-order exponential decay function.

Steroselectivity of *Cp*AR2 for substrate ECOO: The reaction mixture consisted of 20 mM substrate, 20 U of purified *Cp*AR2, 20 U of *Bm*GDH, 30 mM glucose, 0.5 mM $NADP^+$ in 1 mL of Tris-HCl buffer (pH 7.0), with shaking at 30°C for 12 h. Then each of the reaction mixture was extracted with ethyl acetate and the conversion of substrate was determined by GC analysis. The product was acetylated before GC analysis. An appropriate amount of acetic anhydride, 4-dimethylaminopyridine (DMAP) and pyridine was added to the ethyl acetate solution containing the product, and incubated at 30°C for 12 h. The mixture was then diluted properly with ethyl acetate for GC analysis.

GC analysis: The conversion of substrates and enantiomeric excess of products were determined by GC analysis using a Shimadzu GC-2014 gas chromatography, equipped with a CP-Chirasil-Dex CB column (25 m × 0.25 mm × 0.39 mm, Agilent Technologies), a capillary column (30 m length, 0.25 µm film thickness, HP-5MS, Agilent Technologies) and a flame ionization detector (FID). Injection and detection temperatures were set at 280°C, while the oven temperature was fixed at 160°C (Figure S4).

Homology modeling: A homology model of *Cp*AR2 was built based on the crystal structure of a methylglyoxal reductase GRE2 from *Saccharomyces cerevisiae* (PDB entry: 4PVD),[16] which shares 40.5% sequence identity with *Cp*AR2. The three-dimensional structure model of *Cp*AR2 was generated using Modeller 9.11 based on the crystal structure of a yeast methylglyoxal / isovaleraldehyde reductase Gre2 (with 40.5% identity to *Cp*AR2) in complex with NADPH (PDB ID: 4PVD). AutoDock Vina was used for the docking of substrate ECOO into the model structure. All figures of protein models were prepared with PyMOL.[17]

Biocatalytic asymmetric reduction of ECOO: A biocatalytic reaction 10-mL scale was conducted to monitor the reaction time-courses of *Cp*AR2 wild type and its variants. The reaction mixture was composed of substrate ECOO (0.5 M, 110 g L^{-1}), 1.5 equiv. of glucose, 2 g L^{-1} of lyophilized *E. coli* cells co-expressing *Cp*AR2 and *Bm*GDH (*Cp*$AR2_{WT}$: 17.7 U/mg cells; *Cp*$AR2_{S131Y/Q252I}$: 32.1 U/mg cells; *Bm*GDH: 3.5 U/mg cells), 5% ethanol (v/v) or 5% DMSO (v/v) and 0.1 mM $NADP^+$ in Tris-HCl (100 mM, pH 7.0). The mixture was agitated at 30°C-40°C and 500 rpm, and the pH of reaction system was maintained at 7.0 by auto-titrating 1.0 M K_2CO_3 solution. Aliquots of sample (200 µL each) were taken at pre-determined times. The product in the sample was extracted into 200 µL ethyl acetate and the resultant organic phase was dried over anhydrous Na_2SO_4 for the analysis of substrate conversion and product ee by GC.

Acknowledgements

This work was financially supported by the National Natural Science Foundation of China (21878085, 21871085 and 21536004), the National Key Research and Development Program of China (2018YFC1706200), and the Fundamental Research Funds for the Central Universities (22221818014).

Conflict of Interest

The authors declare no conflict of interest.

Keywords: asymmetric synthesis • directed evolution • enzymatic catalysis • ethyl (*R*)-8-chloro-6-hydroxyoctanoate • ketoester reductase • lipoic acid

[1] A. E. Midaoui, J. de Champlain, *Hypertension* **2002**, *39*, 303–307.

[2] M. Morcos, V. Borcea, B. Isermann, S. Gehrke, T. Ehret, M. Henkels, S. Schiekofer, M. Hofmann, J. Amiral, H. Tritschler, R. Ziegler, P. Wahl, P. P. Nawroth, *Diabetes Res. Clin. Pract*. **2001**, *52*, 175–183.

[3] a) G. Raddatz, H. Bisswanger, *J. Biotechnol*. **1997**, *58*, 89–100; b) L. Packer, K. Kraemer, G. Rimbach, *Nutrition* **2001**, *17*, 888–895; c) I. C. Gunsalus, L. S. Barton, W. Gruber, *J. Am. Chem. Soc.* **1956**, *78*, 1763–1766.

[4] I. O. Sutherland, P. C. B Page, C. M. Rayner, EP0261 336 A2, **1988**.

[5] F. Villani, A. Nardi, A. Salvi, G. Falabella, US6670484 B2, **2003**.

[6] a) W. J. Zhou, Y. Ni, G. W. Zheng, H. H. Chen, Z. R. Zhu, J. H. Xu, *J. Mol. Catal. B: Enzym.* **2014**, *99*, 102–107; b) R. Zimmer, U. Hain, M. Berndt, R. Gewald, H.-U. Reissig, *Tetrahedron: Asymmetry* **2000**, *11*, 879–887; c) A. S. Gopalan, H. K. Jacobs, *Tetrahedron Lett.* **1989**, *30*, 5705–5708; d) A. S. Gopalan, H. K. Jacobs, *J. Chem. Soc., Perkin Trans. 1* **1990**, *7*, 1897–1900; e) T. T. Upadhya, M. D. Nikalje, A. Sudalai, *Tetrahedron Lett.* **2001**, *42*, 4891–4893; f) R. Gewald, G. Laban, T. Beisswenger. US5731448 A, **1998**; g) S. P. Chavan, C. Praveen, G. Ramakrishna, U. R. Kalkote, *Tetrahedron Lett.* **2004**, *45*, 6027–6028; h) N. W. Fadnavis, R. L. Babu, S. K. Vadivel, A. A. Deshpande, U. T. Bhalerao, *Tetrahedron: Asymmetry* **1998**, *9*, 4109–4112; i) H. D. Yan, Z. Wang, L. J. Chen, *J. Ind. Microbiol. Biotechnol.* **2009**, *36*, 643–648.

[7] a) M. Olbrich, R. Gewald, US7135328 B2, **2006**; b) M. Müller, W. Sauer, G. Laban, US7157253 B2, **2007**; c) A. Gupta, M. Bobkova, A. Zimmer, EP1685248 B1, **2004**; d) R. J. Chen, G. W. Zheng, Y. Ni, B. B. Zeng, J. H. Xu, Tetrahedron: Asymmetry, **2014**, *25*, 1501–1504.

[8] a) X. M. Gong, G. W. Zheng, Y. Y. Liu, J. H. Xu, *Org. Process Res. Dev.* **2017**, *21*, 1349–1354.; b) Z. M. Cui, J. D. Zhang, X. J. Fan, G. W. Zheng, H. H. Chang, W. L. Wei, *J. Biotechnol.* **2017**, *243*, 1–9; c) N. D. Shen, Y. Ni, H. M. Ma, L. J. Wang, C. X. Li, G. W. Zheng, J. Zhang, J. H. Xu, *Org. Lett.* **2012**, *14*, 1982–1985; d) H. M. Ma, L. L. Yang, Y. Ni, J. Zhang, C. X. Li, G. W. Zheng, H. Y. Yang, J. H. Xu, *Adv. Synth. Catal.* **2012**, *354*, 1765–1772; e) F. Qin, B. Qin, T. Mori, Y. Wang, L. Meng, X. Zhang, X. Jia, I. Abe, S. You, *ACS Catal.* **2016**, *6*, 6135−6140; f) G. W. Zheng, J. H. Xu, *Curr. Opin. Biotechnol.* **2011,** *22*, 784–792; g) P. Wei, J. X. Gao, G. W. Zheng, H. Wu, M. H. Zong, W. Y. Lou, *J. Biotechnol.* **2016**, *230*, 54-62; h) P. Wei, Y. H. Cui, M. H. Zong, P. Xu, J. Zhou, W. Y. Lou, *Bioresour. Bioprocess*, **2017**, *4*, 39; i) Y. J. Wang, X. P. Chen, W. Shen, Z. Q. Liu, Y. G. Zheng, *Biochem. Eng. J.* **2017**, *128*, 54–62.

[9] a) Y. J. Zhang, W. X. Zhang, G. W. Zheng, J. H. Xu, *Adv. Synth. Catal.* **2015**, *357*, 1697–1702; b) J. H. Xu, Y. J. Zhang, G. W. Zheng, J. Pan, US10294479 B2, **2019**.

[10] S. Luetz, L. Giver, J. Lalonde, *Biotechnol. Bioeng.* **2008**, *101*, 647–653.

[11] a) R. A. Sheldon, P. C. Pereira, *Chem. Soc. Rev.* **2017**, *46*, 2678–2691; b) G. Qu, A. T. Li, C. G. Acevedo-Rocha, Z. Sun, M. T. Reetz, *Angew. Chem. Int. Ed.* **2019**, 58, DOI: 10.1002/anie.201901491; c) S. K. Ma, J. Gruber, C. Davis, L. Newman, D. Gray, A. Wang, J. Grate, G. W. Huisman, R. A. Sheldon, *Green Chem.* **2010**, *12*, 81–86; d) C. A. Denard, H. Ren, H. Zhao, *Curr. Opin. Chem. Biol.* **2015**, *25*, 55−64; e) Y. Nie, S. Wang, Y. Xu, S. Luo, Y. L. Zhao, R. Xiao, G. T. Montelione, J. F. Hunt, T. Szyperski, *ACS Catal.* **2018**, *8*, 5145−5152; f) J. Y. Zhou, Y. Wang, G. C. Xu, L. Wu, R. Z. Han, U. Schwaneberg, Y. J. Rao, Y. L. Zhao, J. H. Zhou, Y. Ni, *J. Am. Chem. Soc.* **2018**, *140*, 12645−12654; g) X. M. Gong, Z. Qin, F. L. Li, B. B. Zeng, G. W. Zheng, J. H Xu. *ACS Catal.* **2019**, *9*, 147–153.

[12] K. Chen, F. H. Arnold, *Proc. Natl. Acad. Sci. USA* **1993**, *90*, 5618–5622.

[13] a) G. W. Zheng, Y. Y. Liu, Q. Chen, L. Huang, H. L. Yu, W. Y. Lou, C. X. Li,; Y. P. Bai, A. T. Li, J. H. Xu, *ACS Catal*. **2017**, *7*, 7174–7181; b) F. F. Chen, G. W. Zheng, L. Liu, H. Li, Q. Chen, F. L. Li, C. X. Li, J. H. Xu, *ACS Catal.* **2018**, *8*, 2622−2628.

[14] a) A. Paiardini, G. Gianese, F. Bossa, *Proteins: Structure Function & Bioinformatics* **2003**, *50*, 122–134; b) J. K. Yano, T. L. Poulos, *Curr. Opin. Biotechnol.* **2003**, *14*, 360–365.

[15] S. H. Baik, T. Ide, H. Yoshida, O. Kagami, S. Harayama, *Appl. Microbiol. Biotechnol.* **2003**, *61*, 329–335.

[16] P. C. Guo, Z. Z. Bao, X. X. Ma, Q. Xia, W. F. Li, *Biochim. Biophys. Acta.* **2014,** *1844,* 1486–1492.

[17] L. Schrödinger, The PyMol Molecular Graphics System Schrodinger, Version 1.5, New York, **2012**.

Entry for the Table of Contents (Please choose one layout)

FULL PAPER

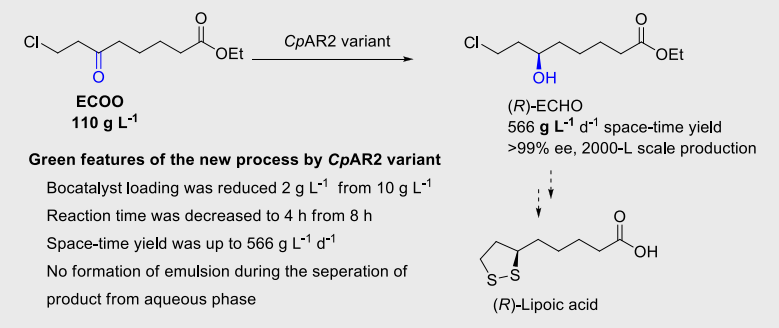

*Yao Xu, Qi Chen, Zhi-Jun Zhang, Jian-He Xu, and Gao-Wei Zheng**

Page No. 1 – Page No. 6

Title

Co-evolving the Activity and Thermostability of an ε-Ketoester Reductase for Better Synthesis of (*R*)-α-Lipoic Acid Precursor